ISSN 1674-1056
http://cpb.iphy.ac.cn
http://iopscience.iop.org/cpb
中国物理 B
Chinese Physics
中国物理 Chinese Physics B

Low-lying electronic states of aluminum monoiodide

Xiang Yuan(袁翔), Shuang Yin(阴爽), Yi Lian(连艺), Pei-Yuan Yan(颜培源), Hai-Feng Xu(徐海峰), Bing Yan(闫冰)

Citation: Chin. Phys. B . 2019, 28(4): 043101. **doi:** 10.1088/1674-1056/28/4/043101
Journal homepage: http://cpb.iphy.ac.cn; http://iopscience.iop.org/cpb

What follows is a list of articles you may be interested in

Potential energy curves, transition dipole moments, and radiative lifetimes of KBe molecule

Ming-Jie Wan(万明杰), Cheng-Guo Jin(金成国), You Yu(虞游), Duo-Hui Huang(黄多辉), Ju-Xiang Shao(邵菊香)
Chin. Phys. B . 2017, 26(3): 033101. **doi:** 10.1088/1674-1056/26/3/033101

MRCI+Q study of the low-lying electronic states of CdF including spin—orbit coupling

Shu-Tao Zhao(赵书涛), Bing Yan(闫冰), Rui Li(李瑞), Shan Wu(武山), Qiu-Ling Wang(王秋玲)
Chin. Phys. B . 2017, 26(2): 023105. **doi:** 10.1088/1674-1056/26/2/023105

Low-lying electronic states of CuN calculated by MRCI method

Shu-Dong Zhang(张树东), Chao Liu(刘超)
Chin. Phys. B . 2016, 25(10): 103103. **doi:** 10.1088/1674-1056/25/10/103103

Ab initio investigation of sulfur monofluoride and its singly charged cation and anion in their ground electronic state

Song Li(李松), Shan-Jun Chen(陈善俊), Yan Chen(陈艳), Peng Chen(陈朋)
Chin. Phys. B . 2016, 25(3): 033101. **doi:** 10.1088/1674-1056/25/3/033101

Ab initio MRCI+Q study on potential energy curves and spectroscopic parameters of low-lying electronic states of CS^+

Li Rui, Wei Chang-Li, Sun Qi-Xiang, Sun Er-Ping, Jin Ming-Xing, Xu Hai-Feng, Yan Bing
Chin. Phys. B . 2013, 22(12): 123103. **doi:** 10.1088/1674-1056/22/12/123103

Low-lying electronic states of aluminum monoiodide*

Xiang Yuan(袁翔), Shuang Yin(阴爽), Yi Lian(连艺), Pei-Yuan Yan(颜培源), Hai-Feng Xu(徐海峰)†, and Bing Yan(闫冰)‡

Jilin Provincial Key Laboratory of Applied Atomic and Molecular Spectroscopy (Jilin University), Institute of Atomic and Molecular Physics, Jilin University, Changchun 130012, *China*

(Received 24 October 2018; revised manuscript received 24 January 2019; published online 5 March 2019)

High-level *ab initio* calculations of aluminum monoiodide (AlI) molecule are performed by utilizing the multi-reference configuration interaction plus Davidson correction (MRCI+Q) method. The core-valence correlation (CV) and spin–orbit coupling (SOC) effect are considered. The adiabatic potential energy curves (PECs) of a total of 13 Λ–S states and 24 Ω states are computed. The spectroscopic constants of bound states are determined, which are in accordance with the results of the available experimental and theoretical studies. The interactions between the Λ–S states are analyzed with the aid of the spin–orbit matrix elements. Finally, the transition properties including transition dipole moment (TDM), Frank–Condon factors (FCF) and radiative lifetime are obtained based on the computed PEC. Our study sheds light on the electronic structure and spectroscopy of low-lying electronic states of the AlI molecule.

Keywords: AlI molecule, potential energy curves (PECs), core-valence correlation, spin–orbit coupling, multi-reference configuration interaction (MRCI)

PACS: 31.15.A–, 33.70.Ca, 31.15.aj **DOI:** 10.1088/1674-1056/28/4/043101

1. Introduction

Aluminum monohalide plays an important role in the astrophysics[1] and molecular laser cooling.[2–6] The spectroscopic constants and the transition properties are critical to the understanding of the chemical and physical processes of these molecules. In recent years, aluminum monohalides have attracted increasing research interest due to their potential applications in molecular laser cooling. Based on the computed potential energy curves (PECs) and the spectroscopic constants, the laser cooling schemes using either AlF[6] or AlCl[4] and AlH,[6] have been suggested theoretically. As for AlBr,[5] however, the feasibility of laser cooling is still under debate,[4,5] owing to the fact that for heavy-atom-contained molecules, the electronic structure and spectroscopic constants are strongly affected with the inclusion of the core–valence correlation (CV) correction and spin–orbit coupling (SOC) effect.

While the spectrum and structure of electronic states have received considerable attention in previous experimental and theoretical investigations for lighter aluminum monohalides (AlF, AlCl, AlBr), our knowledge about AlI is still insufficient, especially for the electronic excited states, due to the abundant inner-shell electrons. To date, the experimental spectroscopic information is only available for the ground electronic state and the first triplet state.[7–9] Theoretically, Varga *et al.*[10] computed the molecular constants of the ground state by couple cluster single and double method combined with a perturbative treatment of triple excitation (CCSD(T)) method. The latest *ab initio* computation was performed by Hamade *et al.*[11] in 2009, in which the PECs and spectroscopic constants of 12 Λ–S states were investigated by using the multi-reference configuration interaction (MRCI) with single and double excitations plus Davidson correction (+Q). To the best of our knowledge, the SOC effect and CV correlation have not been investigated for AlI molecule. It has been indicated that these effects have significant influence on the electronic structures of the diatomic molecules containing heavy atom, such as PbO, ZnH and GeO.[12–14] Furthermore, the SOC effect leads to perturbations for the intercrossing of electronic states, changing the shape of PECs by the avoided crossing phenomenon. As a result, the spectroscopic and dynamic properties of electronic excited states are affected significantly due to the SOC effect.

The goal of this work is to achieve more accurate and detailed electronic structure of AlI molecule. A high-level *ab initio* calculation method using MRCI+Q is employed to compute a total of 13 singlet/triplet Λ–S states correlating with the lowest two dissociation limits of AlI molecule. The CV correction is considered via singly and doubly electron excitation from inner shells, and the SOC interactions between the Λ–S states are evaluated by the *SO* matrix elements. The 13 Λ–S states split into 24 Ω states when the SOC is introduced. The spectroscopic constants of low-lying Λ–S and Ω

*Project supported by the National Key Research and Development Program of China (Grant No. 2017YFA0403300), the National Natural Science Foundation of China (Grant Nos. 11874179, 11574114, and 11874177), and the Natural Science Foundation of Jilin Province, China (Grant Nos. 20180101289JC).

†Corresponding author. E-mail: xuhf@jlu.edu.cn

‡Corresponding author. E-mail: yanbing@jlu.edu.cn

© 2019 Chinese Physical Society and IOP Publishing Ltd

electronic states are obtained based on the computed PECs. We also acquire the transition properties of low-lying states including transition dipole moments (TDM), Frank–Condon factors (FCFs), and radiative lifetimes.

2. Computational details

The *ab initio* calculations of the electronic structure of the AlI molecule are performed with the quantum chemistry MOLPRO 2012 program package.[15] The C_{2v} point group as the Abelian subgroup of the $C_{\infty v}$ has been employed in the calculation of the electronic structure because of the limitation of the MOLPRO program. The C_{2v} point group holds $A_1/B_1/B_2/A_2$ irreducible representation, and the corresponding relationship with $C_{\infty v}$ point group is $\Sigma^+ = A_1$, $\Pi = B_1 + B_2$, $\Delta = A_1 + A_2$, and $\Sigma^- = A_2$, respectively. For the AlI molecule, four a1, two b_1, two b_2 molecule orbitals (MOs) are determined as the active space, which correspond to the atomic orbitals Al 3s3p and I 5s5p.

We calculate 47 single point energies corresponding to the internuclear distance range of 1.9 Å–6.5 Å to obtain the adiabatic PECs of the ground and excited states. In these calculations, the Gaussian-type basis set cc-pwCVQZ-PP[16] in combination with corresponding relativistic effective core potential and cc-pwCVQZ[17] are selected for the I atom and the Al atom, respectively. The process of the calculation contains three steps. First, Hartree–Fock (HF) method is used for obtaining the single-configuration wavefunction of the ground state for the AlI molecule. Then, the state-averaged complete active space self-consistent field (SACASSCF)[18,19] is adopted. In the SACASSCF calculation, we involve a total of 13 electronic states including three $^1\Sigma^+$, two $^1\Pi$, one $^1\Delta$, one $^1\Sigma^-$, two $^3\Sigma^+$, two $^1\Pi$, one $^1\Delta$, and one $^3\Sigma^-$ states. Finally, the MRCI[20] approach is employed to treat the dynamic correlation of the electrons. To balance the accuracy and the cost of the computation, the 4d orbitals of I is placed in the closed shells and correlated with the calculation of electronic correlation energy. In a word, a total of 22 electrons participate in the calculation of electronic correlation energy. The inner electrons of I are taken into account through energy-consistent pseudopotential (ECP) ECP28MDF. The Davidson correction[21] is used to overcome the problem of the size-consistence, which is introduced by the MRCI method.

The spin–orbit coupling effect is handled at the MRCI level. The spin–orbit coupling matrix element is dealt with the help of the state interaction approach via Breit–Pauli operator[22] for Al atom and ECP spin–orbit operator implemented in the ECP of I atom. The off-diagonal spin–orbit matrix elements are calculated at the MRCI level, however the diagonal spin–orbit matrix elements are substituted with MRCI+Q energies. The 13 Λ–S states split into 24 Ω states when we consider the influence of the spin–orbit coupling. The PECs of these 13 Λ–S states and 24 Ω states are depicted following the avoided crossing rule.

According to the PECs of the Λ–S and Ω states, the corresponding spectroscopic constants of the bound states are determined by resolving the one-dimensional nuclear Schrödinger equation with the aid of LEVEL program,[23] including excitation energy T_e, equilibrium internuclear distance R_e, vibrational constants ω_e, and $\omega_e\chi_e$, rotation constant B_e, and vibrational–rotational coupling constant α_e. The dissociation energy D is obtained by deducting the energy at R_e from the energy at a large separation. The transition properties of the AlI molecule, including the TDMs are also evaluated at the MRCI level. Based on the PECs, the FCFs are also determined with the help of the LEVEL program. Finally, based on the TDMs and FCFs, the radiative lifetimes of the several lowest energy transitions are predicted.

3. Result and discussion

3.1. PECs of 13 Λ–S states

The 13 Λ–S states of the AlI molecule, including seven singlet states and six triplet states, are studied by using the MRCI+Q method. Except for $3^1\Sigma^+$ state, which correlates with the ion-pair dissociation limit $Al^+(^1S_g)+I^-(^1S_g)$, all the other Λ–S states correlate with the neutral atomic dissociation limit Al (^2P_u)+I (^2P_u). The adiabatic PECs of Λ–S states are obtained, which are depicted in Fig. 1.

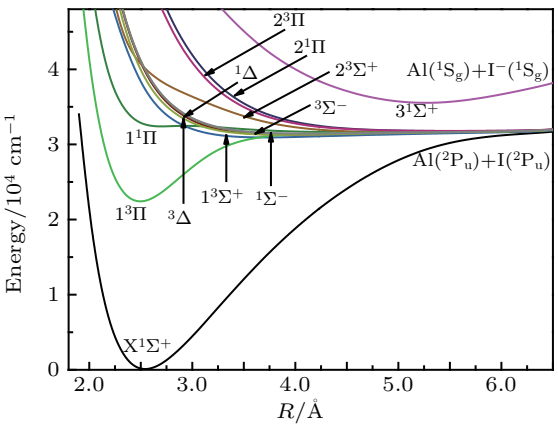


Fig. 1. PECs of Λ–S states for AlI molecule.

As shown in this figure, the $X^1\Sigma^+$ and $1^3\Pi$ states are typical bound states, while the other states are repulsive states or quasi-bound states containing a very shallow potential well. The spectroscopic constants, including T_e, R_e, ω_e, $\omega_e\chi_e$, B_e, and α_e of the bound states are calculated by solving the radial Schrödinger equation of the nuclear motion. The results are listed in Table 1, along with their main electron configurations (CFSs) at R_e.

Table 1. Spectroscopic constants of bound and quasi-bound Λ–S states.

State	R_e/Å	T_e/cm^{-1}	ω_e/cm^{-1}	$\omega_e\chi_e$/cm^{-1}	B_e/cm^{-1}	$10^2\alpha_e$	D/cm^{-1}	CFS at R_e/%	Ref.
$X^1\Sigma^+$	2.5368	0	322.77	0.757	0.1178	0.5395	31659	$15\sigma^2 16\sigma^2 17\sigma 6\pi^4 7\pi$ (81.80)	
	2.5371		316.25 ± 0.02	0.981	0.1177	.5586			Exp[7]
	2.5371	0	316.16 ± 0.02	0.960	0.1177	.5586	30590		Exp[8]
	2.556		311.72	1.08					Cal[11]
	2.534		321.2				33576		Cal[10]
$1^3\Pi$	2.4874	22306.16	338.20	1.94	0.1224	0.6981	9648	$15\sigma^2 16\sigma^\alpha 17\sigma 6\pi^4 7\pi^\alpha$ (83.40)	
		22092.53	332.28	1.671	0.1217	0.6269			Exp[9]
	2.50	22159	331	1.84					Cal[11]
$1^3\Sigma^+$	3.70	30932.72	51.93	0.937	0.0556	.1245	935	$15\sigma^2 16\sigma^2 17\sigma 6\pi^{\alpha\alpha\beta} 7\pi^\alpha$ (82.53)	
$2^3\Sigma^+$	5.09	31643.79	24.17	0.227	0.0296	0.06956	312	$15\sigma^2 16\sigma^2 17\sigma^0 6\pi^{\alpha\alpha\beta} 7\pi^\alpha$ (34.58)	
								$15\sigma^2 16\sigma^\alpha 17\sigma^\alpha 6\pi^4 7\pi^0$(52.51)	
								$15\sigma^0 16\sigma^\alpha 17\sigma^\alpha 6\pi^4 7\pi^2$(2.04)	
$3^1\Sigma^+$	5.27	35528.0	88.76	0.237	0.0273	0.00374-	20510	$15\sigma^2 16\sigma^2 17\sigma 6\pi^4 7\pi$ (63.18)	
								$15\sigma^2 16\sigma^\alpha 17\sigma^\beta 6\pi^4 7\pi$ (21.45)	

So far, only the spectroscopic constants of $X^1\Sigma^+$ and $1^3\Pi$ states of AlI have been reported in previous experimental work. As shown in Table 2, the ground state $X^1\Sigma^+$ of AlI molecule is mainly characterized by the electronic configuration $15\sigma^2 16\sigma 6\pi^4 7\pi$ (81.08%) at R_e. Comparing with the experimental work of Wyse[7] and Martin *et al.*,[8] the deviation of our computed R_e, ω_e is considerable small. In particular, the R_e of this work is closer to CCSD(T)[10] result than MRCI+Q result reported by Hamade *et al.*[11] since in both the former and this work the CV effect is taken into consideration. The first triplet state, $1^3\Pi$, corresponds to the electronic configuration of $15\sigma^2 16\sigma^\alpha 6\pi^4 7\pi^\alpha$ (83.40%) at R_e. The electronic configuration indicates that the $1^3\Pi$ state corresponds to the one-electron $15\sigma \rightarrow 7\pi$ excitation, so does the $X^1\Sigma^+$ state. Compared with the experimental result,[8] the percentage deviation of T_e, and ω_e, are about 1% and 2%, respectively. As for R_e, the difference between our result and Hamade *et al.*'s is smaller than 0.02 Å. Considering different aluminum monohalides AlX (X = F, Cl, Br, I), the R_e of the ground state $X^1\Sigma^+$ increases as the halogen changes from F to I, while the D of $X^1\Sigma^+$ decreases, which indicates that the bonding of aluminum and halogen weakens and the stability of aluminum monohalide decreases. This trend becomes more distinct for the excited state. The first excited singlet state $1^1\Pi$ of AlI molecule is a repulsive one, in contrast to the bound $1^1\Pi$ states of other aluminum monohalides AlX (X = F, Cl, Br). For the $3^1\Sigma^+$ state, the electron configuration shows the remarkable multi-configuration character, composed of $13\sigma^2 14\sigma^2 15\sigma^2 16\sigma 7\pi^4 8\pi$ (63.18%) and $13\sigma^2 14\sigma^2 15\sigma^\alpha 16\sigma^\beta 7\pi^4 8\pi$ (21.45%). As shown in Table 1, the D of the $3^1\Sigma^+$ state is considerably large because the PEC of the $3^1\Sigma^+$ state gradually turns into $1/R$ resulting from the Coulomb interaction between Al^+ and I^-.

Figure 2 shows the permanent dipole moments (PDMs) of $X^1\Sigma^+$, $1^3\Sigma^+$, $2^3\Sigma^+$, $1^3\Pi$, and $3^1\Sigma^+$ states. The AlI molecule is arranged along the z axis, and the origin is located in the center of mass of the AlI molecule. The positive direction points from Al to I. It can be seen that all the calculated PDMs at large internuclear distance are close to zero a.u. except for PDM of the $3^1\Sigma^+$ state. The variation of PDM of the electronic states can reflect the ionic characteristics of these states. The center of positive charges with the position vector λ is set to be at zero, corresponding to the dissociation limit of neutral atoms. The PDM of the $X^1\Sigma^+$ and $1^3\Pi$ state have a negative peak at about $R = 4.4$ Å and $R = 2.9$ Å, respectively. The PDM of the $3^1\Sigma^+$ state is negative and becomes linearly-dependent R when R is larger than 5.0 Å, which is attributed to the fact that the dissociation limit of the $3^1\Sigma^+$ state comes from ion-pair $Al^+(^1S_g)+I^-(^1S_g)$. There is a suddenly complementary change of the dipole moment for each of the $1^3\Sigma^+$ and $2^3\Sigma^+$ state at about $R = 2.3$ Å, which may be due to the avoided crossings. To clarify this, we show in Table 2 the main electric configurations of $1^3\Sigma^+$ and $2^3\Sigma^+$ states with the R in a range of 2.2 Å–2.5 Å. It can be seen from the table, the main electronic configurations of $1^3\Sigma^+$ and $2^3\Sigma^+$ states are exchanged near $R = 2.4$ Å, indicating the wave functions of the $1^3\Sigma^+$ and $2^3\Sigma^+$ states are exchanged, which leads to the changes of the PDMs.

Table 2. Main electric configurations of $1^3\Sigma^+$ and $2^3\Sigma^+$ states.

	$15\sigma^2 16\sigma^\alpha 17\sigma^\alpha 6\pi^4 7\pi$		$15\sigma^2 16\sigma^2 17\sigma 6\pi^{\alpha\alpha.\beta} 7\pi^\alpha$	
R/Å	$1^3\Sigma^+$	$2^3\Sigma^+$	$1^3\Sigma^+$	$2^3\Sigma^+$
2.2	79.82%	0	4.25%	85.00%
2.3	72.01%	0	11.29%	85.30%
2.4	2.16%	0	83.4%	85.45%
2.5	0	81.94%	85.68%	0
2.6	0.16%	81.75%	85.62%	0.17%
2.7	0.43%	81.54%	85.53%	0.45%

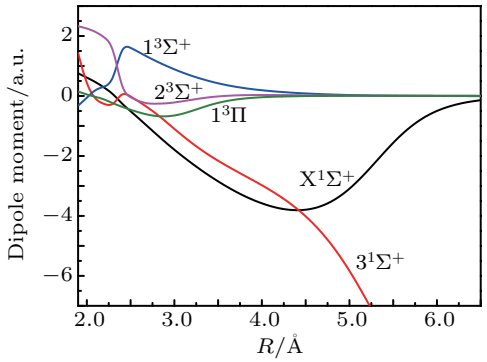


Fig. 2. Dipole moments of five Λ–S states.

3.2. SOC effect on the AlI molecule

For the heavy molecule AlI, the effect of the SOC may not be neglected. The SOC effect causes the Λ–S states to split and mix with common Ω symmetry. From Fig. 1, we can see that the PEC of the $1^3\Pi$ state crosses other states at energy of 30500 cm^{-1}–32000 cm^{-1} in an R range of 3.5 Å–5.5 Å. The $1^3\Pi$ state crosses $1^3\Sigma^+$, $^3\Delta$, $^1\Delta$, $2^1\Sigma^+$, $^1\Sigma^-$, $^3\Sigma^-$, $1^1\Pi$, and $2^3\Sigma^+$ states, with the crossing points located at a high vibrational level ($\upsilon' > 33$).

To analyze the interaction between the $1^3\Pi$ state and other states in detail, the *SO* matrix elements as listed in Table 3 are computed. The calculated *SO* matrix elements versus internuclear distance are plotted in Fig. 3. The spin–orbit operator is represented in the basis of the real spin-electronic function denoted as $|SO_x\rangle$.[24] We find that the absolute values of *SO* matrix element involving $1^3\Pi$ state are all about 1200 cm^{-1} in the region where $1^3\Pi$ state is close to other states. This result suggests that the spin–orbit effect between the excited states of AlI molecule is significant.

Table 3. *SO* matrix elements of Λ–S state.

Spin–orbit matrix elements
$SO_1 = -\mathrm{i}\langle 1^3\Sigma^+\|H_{SO}\|1^3\Pi\rangle_x$
$SO_2 = -\mathrm{i}\langle 1^3\Pi\|H_{SO}\|^3\Delta\rangle_x$
$SO_3 = -\mathrm{i}\langle {}^1\Delta\|H_{SO}\|1^3\Pi\rangle_x$
$SO_4 = -\mathrm{i}\langle 2^1\Sigma^+\|H_{SO}\|1^3\Pi\rangle_y$
$SO_5 = -\mathrm{i}\langle {}^1\Sigma^-\|H_{SO}\|1^3\Pi\rangle_x$
$SO_6 = -\mathrm{i}\langle 1^3\Pi\|H_{SO}\|^3\Sigma^-\rangle_y$
$SO_7 = -\mathrm{i}\langle 1^1\Pi\|H_{SO}\|1^3\Pi\rangle_z$
$SO_8 = -\mathrm{i}\langle 2^3\Sigma^+\|H_{SO}\|1^3\Pi\rangle_x$

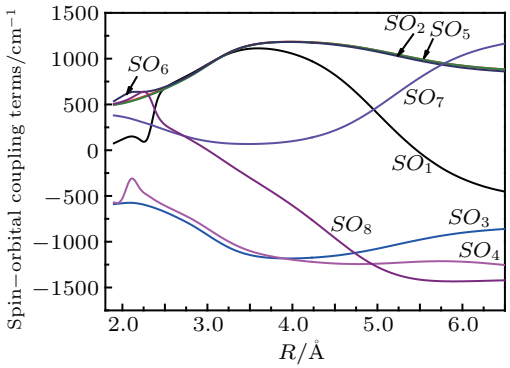


Fig. 3. *R* dependent *SO* matrix elements of several Λ–S states.

3.3. PECs of 24 Ω states

As discussed earlier, the SOC effect plays an important role in AlI molecule. After considering the SOC effect, the 13 Λ–S states split into 24 Ω states, including six states of $\Omega = 0^+$, five states of $\Omega = 0^-$, eight states of $\Omega = 1$, four states of $\Omega = 2$, and one state of $\Omega = 3$. The dissociation limits split into five asymptotes, including Al($^2P_{1/2}$)+I($^2P_{3/2}$), Al($^2P_{3/2}$)+I($^2P_{3/2}$), Al($^2P_{1/2}$)+I($^2P_{1/2}$), Al($^2P_{3/2}$)+I($^2P_{1/2}$), and Al$^+$(^{1}S)+I$^-$(^{1}S). The detailed dissociation relationships of Ω states are listed in Table 4. The energy interval of Al($^2P_{1/2}$)-Al($^2P_{3/2}$) and I($^2P_{3/2}$)–I($^2P_{1/2}$) are calculated to be 128.698 cm^{-1} and 7274.12 cm^{-1}, respectively, which are close to the experimental results 112.061 cm^{-1} and 7715.211 cm^{-1}.[25,26] As for the ion-pair Al$^+$(^{1}S)+I$^-$(^{1}S), we estimate the $1/R$ Coulomb compensation from $R = 6.5$ Å to infinite distance. The computational value of the Al$^+$(^{1}S)+I$^-$(^{1}S) is 3074 cm^{-1} higher than experimental result, which maybe results from the fact that the $R = 6.5$ Å is not far enough to treat the AlI molecule as two independent ions. According to the rules of avoided crossing, the PECs of 24 Ω states are depicted in Fig. 4. Basically, under adiabatic approximation, the rule of avoided crossing requires the two electronic states with the same species (same Ω quantum number in this work) to avoid crossing since the only remaining good quantum number in the diatomic molecule is Ω when the SOC effect is taken into account. The spectroscopic constants of the bound states determined by the PECs are listed in Table 5. In order to compare the Ω states with corresponding Λ–S states evidently, figure 5 shows the R dependent Λ–S components of some low-lying Ω states.

Table 4. Dissociation limit relationships of Ω states.

Ω states	Atomic state	Energy/cm^{-1}	
		Calc.	Expt.
2, 1, 1, X0$^+$, 0$^-$	Al($^2P_{1/2}$)+I($^2P_{3/2}$)		
3, 2, 2, 1, 1, 1, 0$^+$, 0$^+$, 0$^-$, 0$^-$	Al($^2P_{3/2}$)+I($^2P_{3/2}$)	128.698	112.061[a]
1, 0$^+$, 0$^-$	Al($^2P_{1/2}$)+I($^2P_{3/2}$)	7274.12	7603.15[b]
2, 1, 1, 0$^+$, 0$^-$	Al($^2P_{3/2}$)+I($^2P_{1/2}$)	7368.343	7715.211
0$^+$	Al$^+$(^{1}S)+I$^-$(^{1}S)	26682	23608[c]

[a]Ref. [25], [b]Ref. [26], [c]Ref. [27].

The ground Ω state X$^+$ almost completely originates from the Λ–S state X$^1\Sigma^+$. Hence, the spectroscopic constants are also close to the Λ–S state X$^1\Sigma^+$. Nevertheless, the D of X0$^+$ state is about 2244 cm^{-1} smaller than that of the corresponding Λ–S state. Our calculation shows that the energy difference between the X$^1\Sigma^+$ state and the X0$^+$ state is about 90.6 cm^{-1} and 2336.2 cm^{-1} at R_e and $R = 6.5$ Å, respectively. This arises from the fact that the SOC splitting of I atom is significant at atomic limit, and also consistent with the scenario in Fig. 5, in which the component of repulsive state $2^3\Pi$ increases obviously in the range of $R > 4.5$ Å. For the $1^3\Pi$ state, after considering the SOC effect, the (2)0$^+$, (1)1,

(1)0^-, and (1)2 state are generated. The interval of $^3\Pi_{0+}$–$^3\Pi_1$ is 229 cm^{-1}, which is in reasonable agreement with experimental value 201 cm^{-1}.[18] The electric dipole transitions of (1)0^-–X^+ and (1)2–X^+ are forbidden, thus only other two transitions can be observed experimentally. Comparing with the $1^3\Pi$ state, the R_e values of these four Ω states are larger. The T_e values of (2)0^+, (1)1, and (1)0^- reduce 336.8 cm^{-1}, 107.2 cm^{-1}, and 57.4 cm^{-1} respectively, and the T_e of (1)2 increases 207.4 cm^{-1}. As shown in Fig. 5, the Λ–S components of the (2)0^+, (1)0^-, (1)1, and (1)2 states are complicated. For example, the Λ–S components of the (1)1 state are the mixture of the $1^3\Pi$, $^3\Sigma^-$, $1^3\Sigma^+$, and $1^1\Pi$ states in the region of R from 3.5 Å to 4.5 Å, indicating the complicated SOC interaction between these Λ–S states (see Fig. 3).

For the Ω states in the higher energy region, complicated state-mixing and interactions are presented under the influence of the SOC effect. Their PECs are very complex with many avoided crossing points. The (4)0^+ and (5)0^+ state hold the avoided crossing point around $R = 3.6$ Å. Turing to the (5)1 and (6)1 state, there is an avoided crossing point at about $R = 3.3$ Å. This generates a small potential well of (6)1 state. The state $\Omega = 3$ is purely generated from the $^3\Delta$ state, therefore, the shape of the PEC for $\Omega = 3$ is similar to that of the corresponding Λ–S state. Most of Ω states have shallow potential wells, but the depths of these wells are still too shallow to support many vibration levels and their R_e values deviate significantly from that of the X0$^+$ state. So, it can be expected that the spectra of the AlI in this energy range will be very diffuse and these states are hard to observe experimentally.

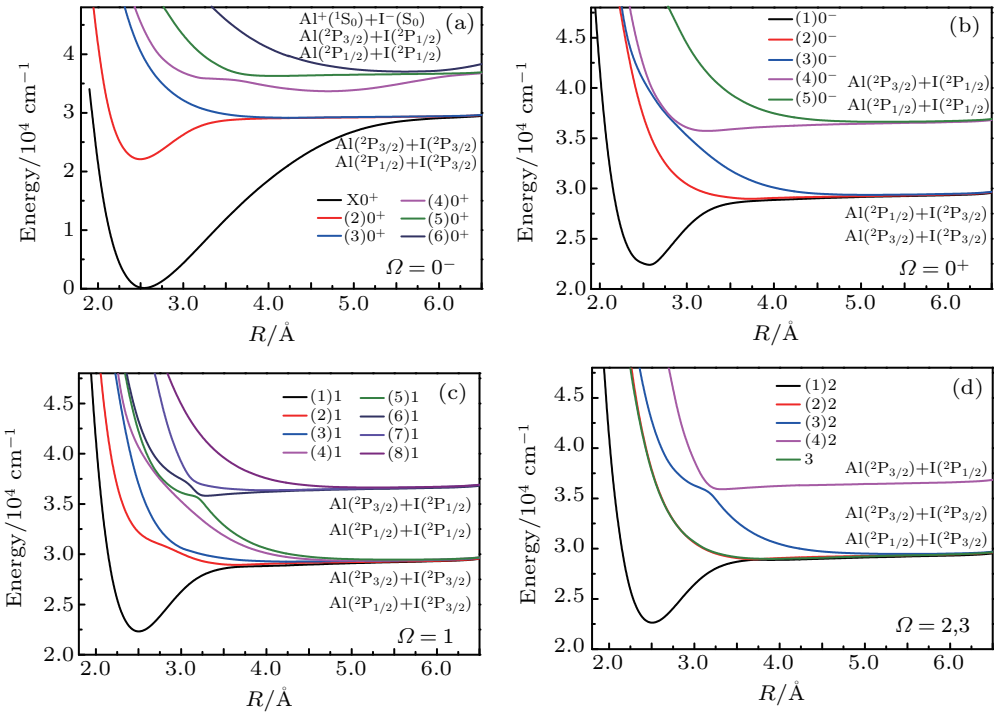


Fig. 4. PECs of a total of 24 Ω states.

Table 5. Spectroscopic constants of several bound Ω states.

Ω state	T_e/cm^{-1}	R_e/Å	ω_e/cm^{-1}	$\omega_e\chi_e$/cm^{-1}	B_e/cm^{-1}	$1^2\alpha_e$/cm^{-1}	D/cm^{-1}	Reference
X0$^+$	0	2.5359	322.5	0.97	0.118	0.059	29256.6	
(2)0$^+$	21969.3	2.4883	335.9	2.29	0.122	0.075	7474.4	
	21892.1	2.4795	337.0	1.77	0.123	0.074		Expt.[8]
(1)1	22198.9	2.4939	331.9	2.42	0.122	0.078	7176.5	
	22092.7	2.4825	333.4	1.84	0.123	0.073		Expt.[8]
(1)0$^-$	22248.8	2.5849	328.6	2.82	0.113	-0.14	7088.0	
(1)2	22513.9	2.4983	329.1	2.51	0.121	0.08	6858.0	

3.4. TDMs, FCFs, and radiative lifetimes of AlI molecule

The transition dipole moments containing (2)1–X0$^+$, (1)1–X0$^+$, and (2)0$^+$–X0$^+$ are calculated each as a function of R in range from 1.9 Å to 6.5 Å. The corresponding functions of TDMs are depicted in Fig. 6. As illustrated in this figure, the absolute TDM value of the (2)1–X0$^+$ transition is much larger than those of (1)1–X0$^+$ and (2)0$^+$–X0$^+$ in the Frank–Condon region. This can be understood as the fact that

the main Λ–S components of (2)1 state is $1^1\Pi$ state, whose transition to $X^1\Sigma^+$ is spin-allowed. The reason why the TDM values of (2)1–X0$^+$ decreases rapidly as R increases is that the Λ–S components of (2)1 state changes from $1^1\Pi$ state to other triple states near $R = 2.5$ Å as shown in Fig. 5. The transition (1)1–X0$^+$ and (2)0$^+$–X0$^+$ mainly originates from the spin-forbidden transition $1^3\Pi$–$X^1\Sigma^+$. However, the transition intensity of (2)0$^+$–X0$^+$ is much larger than that of (1)1–X0$^+$, because the former transition comes from the spin-allowed $2^1\Sigma^+$–$X^1\Sigma^+$ component.

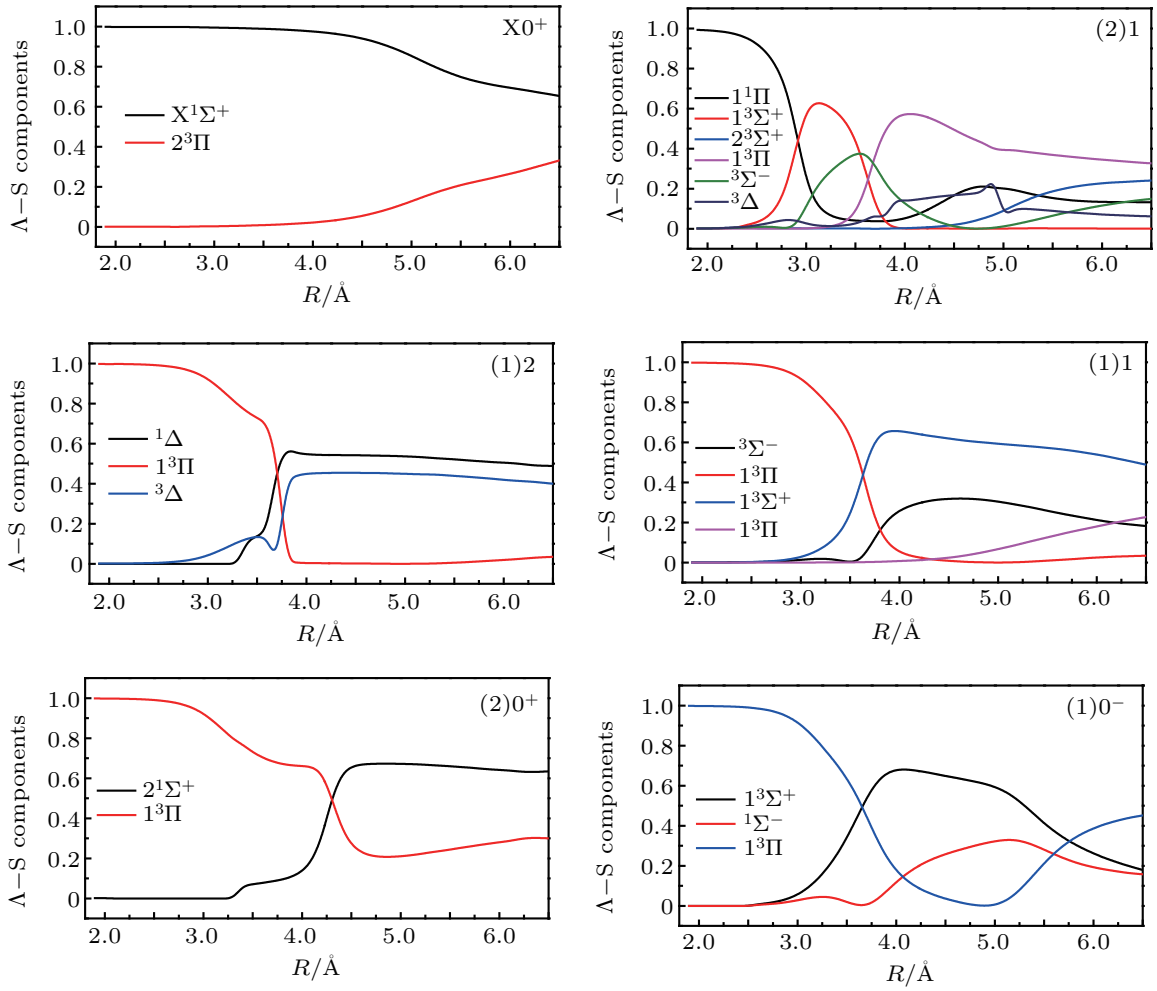


Fig. 5. Curves of Λ–S component *versus* R of X0$^+$, (1) 0$^-$, (2)0$^+$, (1)1, (1)2, and (2)1 states.

The Frank–Condon factors of the (1)1–X0$^+$ and (2)0$^+$–X0$^+$ are calculated with the aid of LEVEL program as listed in Table 6. It can be seen from Table 6 that the $\Delta v = v' - v'' = 0$ bands of (1)1–X0$^+$ and (2)0$^+$–X0$^+$ transition are more intense than the other bands, indicating that (1)1, (2)0$^+$, and X0$^+$ state have similar equilibrium internuclear distances. For the aforementioned transitions, the radiative lifetime τ of the vibration level v' for a specified state is defined as the inverse of the total transition probability

$$\tau_{v'} = (A_{v'})^{-1} = \frac{4.9355 \times 10^5 g'}{\left(\sum_{v''} q_{v'v''} \Delta E^3_{v'v''}\right) \times |TDM|^2},$$

where g' is the degeneracy of the upper state, $q_{v'v''}$ is the Frank–Condon factor of the two vibrations levels, the energy difference $\Delta E_{v'v''}$ is in unit of cm^{-1}, and TDM (in atomic unit) is the average electronic transition dipole moment. The results of the radiative lifetimes are listed in Table 7. The computed radiative lifetimes of (2)0$^+$ and (1)1 are 21 μs and 95 μs, respectively.

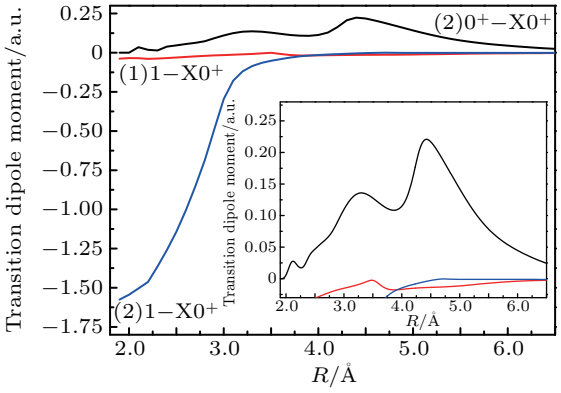


Fig. 6. Transition dipole moments of AlI molecule.

Table 6. Franck–Condon factors of transitions $(2)0^+$–$X0^+$ and $(1)1$–$X0^+$.

	$v''=0$	1	2	3	4	5	6	7	8	9
					$(2)0^+$–$X0^+$					
$v'=0$	0.800812	0.169654	0.025619	0.003395	0.000446	0.000063	0.000010	0.000001	0.000000	0.000000
1	0.186576	0.499057	0.242683	0.058713	0.010839	0.001786	0.000290	0.000048	0.000007	0.000001
2	0.012423	0.300470	0.304118	0.264903	0.090999	0.021749	0.004360	0.000804	0.000145	0.000025
3	0.000187	0.030287	0.374412	0.174908	0.257189	0.117814	0.034819	0.008266	0.001713	0.000334
4	0.000001	0.000525	0.052134	0.419937	0.092483	0.231784	0.137453	0.048480	0.013313	0.003086
5	0.000000	0.000005	0.001014	0.076528	0.444754	0.043843	0.197953	0.149229	0.061183	0.019136
					$(1)1$–$X0^+$					
$v'=0$	0.845436	0.135274	0.017060	0.001960	0.000234	0.000032	0.000005	0.000001	0.000000	0.000000
1	0.148347	0.599785	0.203765	0.040542	0.006439	0.000951	0.000145	0.000023	0.000003	0.000000
2	0.006191	0.249937	0.427364	0.235228	0.065152	0.013268	0.002371	0.000404	0.000071	0.000012
3	0.000021	0.014951	0.326009	0.300623	0.243033	0.087807	0.021854	0.004619	0.000881	0.000166
4	0.000004	0.000040	0.025716	0.383799	0.208326	0.234057	0.107016	0.031340	0.007664	0.001629
5	0.000000	0.000013	0.000049	0.037717	0.427252	0.143923	0.214063	0.121608	0.040652	0.011317

Table 7. Radiative lifetimes of the transitions $(2)0^+$–$X0^+$ and $(1)1$–$X0^+$.

Transition	Unit	Radiative lifetimes					
		$v'=0$	$v'=1$	$v'=2$	$v'=3$	$v'=4$	$v'=5$
$(2)0^+$–$X0^+$	μs	21.6	21.5	21.5	21.4	21.4	21.5
$(1)1$–$X0^+$	μs	95.18	95.02	94.94	94.89	94.89	95.11

4. Conclusions

The *ab initio* calculations of the AlI molecule have been accomplished with the MRCI+Q method. The PECs of the 13 Λ–S states are calculated, which are related to the two dissociation limits $Al(^2P_u)+I(^2P_u)$ and $Al^+(^1S_g)+I^-(^1S_g)$. Based on the PECs, the spectroscopic constants are determined by resolving the radial Schrödinger equation of the nuclear motion and found to be in good agreement with previous experimental results. The calculated PECs show that the $1^3\Pi$ state crosses with other excited states and the *SO* matrix element indicates that the SOC effect is non-negligible for AlI molecule. After considering the SOC effect, a total of 13 Λ–S states split into 24 Ω states. The potential well of $X0^+$ state is shallower than that of the $X^1\Sigma^+$ state when considering SOC effect. The TDMs, Franck–Condon factors and radiative lifetimes are also determined. Our study exhibits a considerably accurate and detailed electronic structure and spectroscopic information of the AlI molecule by considering the SOC effect and CV correlations, which plays a prominent role in the electronic structure of molecules containing heavy atoms. These results will be helpful for future experimental and theoretical investigations into the structure and dynamic study of aluminum monoiodide.

Acknowledgment

The authors thank the High Performance Computing Center of Jilin University for computing time.

References

[1] Cernicharo J and Guélin M 1987 *Astron. Astrophys.* **183** L10
[2] Shuman E S, Barry J F and Demille D 2010 *Nature* **467** 820
[3] Rosa M D D 2004 *Eur. Phys. J. D.* **31** 395
[4] Yang R, Tang B and Gao T 2016 *Chin. Phys. B* **25** 043101
[5] Liu X T, Shi D D, Shan S M, Yan P Y, Xu H F and Yan B 2016 *J. Phys. Chem. A* **120** 8786
[6] Wells N and Lane I C 2011 *Phys. Chem. Chem. Phys.* **13** 19018
[7] Wyse F C and Gordy W 1972 *J. Chem. Phys.* **56** 2130
[8] Martin E and Barrow R F 1978 *Phys. Scr.* **17** 501
[9] Mahieu E, Dubois I and Bredohl H 1990 *J. Mol. Spectrosc.* **143** 359
[10] Hargittai M and Varga 2010 *J. Phys. Chem.* **111** 6
[11] Hamade Y, Taher F and Monteil Y 2009 *Int. J. Quantum Chem.* **110** 1030
[12] Luo W, Li R, Gai Z Q, Ai R B, Zhang H M, Zhang X M and Yan B 2016 *Chin. Phys. B* **25** 073101
[13] Zhao S T, Liang G Y, Li R, Li Q N, Zhang Z G and Yan B 2017 *Acta Phys. Sin.* **66** 063103 (in Chinese)
[14] Liu X J, Miao F J, Li R, Zhang C H, Li Q N and Yan B 2015 *Acta Phys. Sin.* **64** 123101 (in Chinese)
[15] Werner H J, Knowles P J, Knizia G, Manby F R and Schütz M 2012 *Wires. Comput. Mol. Sci.* **2** 242
[16] Peterson K A and Yousaf K E 2010 *J. Chem. Phys.* **133** 174116
[17] Peterson K A and Dunning T H J 2002 *J. Chem. Phys.* **117** 10548
[18] Werner H J and Knowles P J 1985 *J. Chem. Phys.* **82** 5053
[19] Werner H J and Meyer W 1980 *J. Chem. Phys.* **73** 2342
[20] Werner H J and Knowles P J 1988 *J. Chem. Phys.* **89** 5803
[21] Langhoff S R and Davidson E R 1974 *Int. J. Quantum Chem.* **8** 61
[22] Berning A, Schweizer M, Werner H J, Knowles P J and Palmieri P 2000 *Mol. Phys.* **98** 1823
[23] Le Roy R J 2017 *J. Quantum Spectrosc. Radiat. Transfer* **186** 167
[24] Khalil H, Quéré F L, Brites V and Léonard C 2012 *J. Mol. Spectrosc.* **27** 1
[25] Martin W C and Zalubas R 1979 *J. Phys. Chem. Ref. Data* **8** 817
[26] Luc-Koenig E, Morillon C and Vergès J 1975 *Phys. Scr.* **12** 199
[27] Peláez R J, Blondel C, Delsart C and Drag C 2009 *J. Phys. B: At. Mol. Opt. Phys.* **42** 125001